

Clump formation due to the gravitational instability of a multiphase medium in a massive protoplanetary disc

V. N. Snytnikov^{*} and O. P. Stoyanovskaya

Bereskov Institute of Catalysis SB RAS, Novosibirsk, Lavrentieva, 5, 630090, Russia

Accepted ***. Received ***; in original form ***

ABSTRACT

Planetary systems form in gas-dust protoplanetary discs via the growth of solid bodies. In this paper, we show that the most intriguing stage of such growth — namely, the transformation of 1-10 m boulders into kilometre-sized planetesimals — can be explained by a mechanism of gravitational instability. The present work focused on the origin of self-gravitating clumps in which planetesimal formation could take place. Our computer simulations demonstrated that such clumps of gas and boulders formed due to the development of a two-phase instability. This instability revealed a so-called ‘mutual influence effect’ in the protoplanetary disc, where the dynamics of the system were determined by the collisionless collective motion of a low-mass subdisc composed of primary solids. We found that a $0.1 c_s$ velocity dispersion in the boulder subdisc was sufficient to cause the formation of self-gravitating clumps of gas and boulders. In such regimes, the time needed for the formation of the collapsing objects was less than the boulders’ dissipation time in the density waves of the medium.

Key words: accretion, accretion discs – gravitation – instability – stars: formation – planetary systems: protoplanetary discs.

1 INTRODUCTION

Results from numerical modelling and observations of the gas-dust discs around young solar-type stars provide the basis for the currently accepted scenario for the formation of the Solar System (Hartmann 2009). This model suggests that the disc forms simultaneously with a protostar, following the gravitational collapse of gas in the molecular cloud (Petit & Morbidelli 2005). In the first stage (which lasts up to 100,000 years), a protostar forms; this consists mainly of hydrogen and helium, and has a mass of about one tenth of the solar mass.

The massive gas-dust disc is formed by the collision of the opposing gas streams. The gas streaming during the molecular cloud collapse is supersonic (Spitzer 1978). The infalling gas streams collide and produce the diverging shock waves (Landau & Livshitz 1987) that decelerate the gas streams velocity (see Fig. 1a). Between a pair of shock waves the gas density is higher than its extreme value for a single shock wave, as it was shown theoretically and experimentally by Orishich, Ponomarenko & Snytnikov 1989. When the flow rate of collapsing gas decreases in the end of the star formation stage, the shock waves diverge from the disc plane (see Fig. 1b). Now the gas can leave the disc.

Fast diminution of its flow provides conditions for the fast gas expansion which is followed up with its cooling.

The molecular cloud dust moves together with the gas. During the gas compression behind the shock waves (Fig. 1a) the dust grains grow in size as a result of heavy molecular absorption and coagulation (Cuzzi & Weidenschilling 2006). Adsorption time is less than 10^6 years in a medium with the hydrogen concentration higher than 10^4 cm^{-3} (Spitzer 1978). In the disc the concentration of gas is by several orders of magnitude higher than 10^4 cm^{-3} . So the molecules are adsorbed according to their sublimation temperature. Spitzer (1978) estimated that the coagulation length exceed the absorption length in the order of 1-2. These lengths are significantly less than the massive disc thickness. That is why the dust grains can grow in size in accretion disc, settle on the disc plane and form their own subdisc (Cuzzi & Weidenschilling 2006). Due to the subdisc gas expansion in outside flow the relation of solid density to gas density increases in contrast to the molecular clouds, where dust constitutes 1-2 per cent of the mass.

The protostar increases its mass up to the star mass due to accretion from the disc and the residues of the surrounding molecular cloud. Alteration of the disc mass is defined by the flows: (a) falling to the disc from the cloud, (b) accreting from the disc to the protostar, (c) leaving the disc, e.g. in jets. By the time discs become observable (1-3 million

^{*} E-mail: snyt@catalysis.ru (VNS); stop@catalysis.ru (OPS)

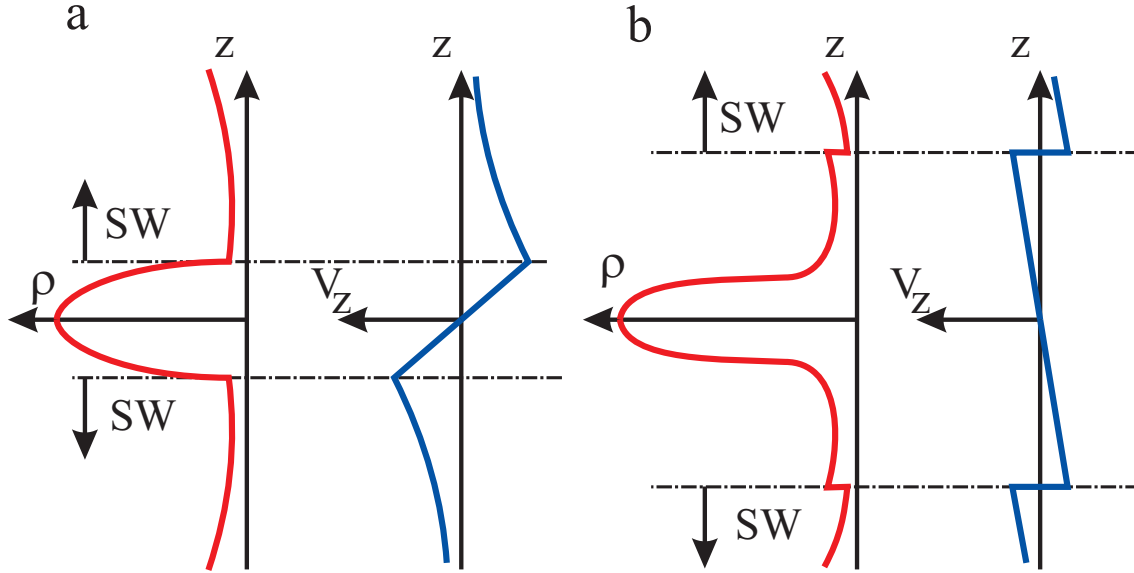


Figure 1. : The formation of the massive gas-dust disc by the collision of the opposing streams during the molecular cloud collapse.

years), their masses have decreased to 1 per cent of the host star mass. Inside the period between protostar and young star a stage of massive disc exists, when the mass of the disc and the mass of the central body are comparable. Over the course of the next 60-100 million years, the circumsolar disc evolves to a state similar to that currently present in our own Solar System.

The formation of planets in circumstellar discs proceeds via the growth of solids; nanometer-sized dust in molecular clouds transforms into planets with radii of some thousands of kilometres.

The growth of dust grains via coagulation depends on chemical composition. Usually ice, silicates and iron are mentioned as dust compounds. But due to the cosmic abundance of chemical elements (Lodders & Fegley 1998) the main components of disc solids must be organic compounds from H, C, O, N with high molecular weights (Herbst & van Dishoeck 2009). Such compounds can be easily synthesized on Mg, Si, O, Fe dust grains that work as catalysts in a medium with abundance of H and He (Khassin & Snytnikov 2005). That is why conglutination of multi-component organic compounds and non-organic bodies can be expected up to 1-10 meter in size. When the subdisc consists of such bodies with velocities greater than 10 km s^{-1} they collide less than once per orbital time.

The growth of planetesimals (i.e., bodies with a size in excess of a kilometre) may occur due to collisional accumulation, since their own gravitational field can attract smaller bodies and hold these to their surface (Safronov 1969). The mechanism by which kilometre-sized planetesimals are formed from 'boulders' (or agglomerates, with sizes from 1 – 10 m) has been the subject of intense interest and discussion, and has formed the basis of many studies (Youdin & Shu 2002, Makalkin & Ziglina 2004, Rice et al. 2006, Johansen et al. 2007). At this stage, the concentration of solids provides motion, with rare collisions at orbital time with velocities of tens kilometers per second. The metre-sized boulders are not enlarged during high-velocity collisions. Collisions of such boulders don't result in sticking irrespective of

their composition. During collisions where the relative velocities exceed 1 m s^{-1} , inorganic compound solids larger than 10 cm are destroyed, rather than sticking together and becoming a larger, aggregate body (Marov et al. 2008). In addition, in circumstellar discs, the time taken for a metre-sized solid to fall to the central body is of the order of 100 years, due to gas drag. Thus, the growth of such solids in the disc may take only some tens of rotations (Wiedenschilling 2000, Armitage 2006). If the growth goes slower, the protoplanetary disc will lose a large proportion of its 'solid' matter, which is the material needed for the formation of Earth-group planets, and asteroids and comets.

The formation of planetesimals can occur either in a massive circumstellar disc (age 0.1-1 million years, with the mass of the disc comparable to that of the central body) or in a medium-mass disc (age exceeding 1 million years, with the mass of the disc an order of magnitude less than the mass of the central body).

One possible way to rapidly assemble metre-sized boulders into a body of planetesimal size could be via gravitational instabilities triggered by the collective motion of the solids subdisc.

Gravitational instability in discs with a central body has been investigated since the 1950s (Edgeworth 1949). It was found that to experience local Jeans instability, a disc with a central body needs lower dispersions in the velocities of solids (Gurevich & Lebedinsky, 1950), as well as lower gas temperatures (Safronov 1960) or higher-density matter (as compared with a motionless medium). Such conditions — which are close to those that trigger other instabilities in the disc (Fridman 2008) — may lead to the formation of rings, spirals, complex wave structures or individual clumps (Snytnikov et al. 2004). The formation of clumps in a rotating medium is hindered by gas heating, as well as the increasing velocity dispersion of solids produced by gravitational field perturbations in spiral and other wave structures. The non-linear behaviour of instabilities and the appearance of clumps (whose densities increase under self-gravitation) are therefore of interest. In any case, for discs to experi-

ence fragmentation, they should be quite dense and cold. Scenarios for the development of instabilities (Levin 1965, Goldreich & Ward 1973) suggest that stable discs transform into unstable ones due to the sedimentation of solids on the equatorial plane. For instability development it was necessary to provide the surface density of the primary solids critical for this particle velocity dispersion. However, the formation of a dense primary solids subdisc is prevented by solids scattering, which is caused by turbulent gas flows resulting from hydrodynamic instability of the Kelvin-Helmholtz type (Cuzzi, Dobrovolskis & Champney 1993). This instability arises because both components of the two-phase subdisc located in the equatorial plane rotate at the Keplerian velocity, whereas the angular velocity of gas outside the plane is lower, due to the radial pressure gradient. A substantial difference in subdisc thickness (with respect to the gas and condensed phases) is not therefore expected.

On the other hand, a disc can reach its instability threshold not only by increasing its density, but also via a decrease in temperature. The main problem with implementing this mechanism in a medium-mass disc is that the lowering of the gas temperature in the disc is accompanied by a rapid formation of spiral structures, which do not transform into clumps. According to estimates made by Makalkin & Ziglina (2004) and Marov et al. (2008), at the stage of planetesimal formation in the Solar System, the temperature of the gas component in the disc at the Earth's radius was 500-700 K when the disc had uniformly distributed solids, and 250-500 K after the formation of a thin subdisc of primary solids. Spiral waves appear at higher temperatures in the medium-mass disc. In these spirals, the dispersion in the velocities of solids increases (Rice et al. 2004). These structures — which result from the development of gravitational instability in the gas — scatter the subdisc of primary solids with sizes exceeding 1 m (Rice et al. 2006). Rapid cooling, which typically occurs in a time comparable to the time taken for the disc rotation, was considered to be a necessary condition for clump formation in such a disc (Gammie 2001, Rice et al. 2003). This imposes stringent restrictions on the mass and temperature of the disc, as well as on the zones of formation of such clumps (Rafikov 2009). Further studies revealed that such restrictions could not provide conclusive evidence, proving — or disproving — that gravitational instability is the mechanism responsible for the formation of large bodies in the discs. The reason is that the critical time of cooling depends on the γ - constant ratio of the specific heats (Rice et al. 2005), the history and rate of cooling (Clarke, Harper-Clark & Lodato 2007), and the ratio of the mass of the disk to the mass of the central body (Meru & Bate 2010). Thus, for a disc whose mass is 10 times smaller than that of the central body, a cooling time equal to 15 disc rotations is now taken to be critical (Lodato & Clarke 2011). However, in the case of a medium-mass disc, such gas cooling conditions can hardly be expected to occur, due to the growing radiation from the star.

The mechanisms that facilitate the formation of planetesimals from large bodies have previously been studied for medium-mass discs. According to the computer simulation made by Rice et al. (2004, 2006) for a two-phase disc, metre-sized solid particles can concentrate in spiral arms for some time, due to gas dragging. Computational experiments by Youdin & Shu (2002) demonstrated that a turbulent gas

flow resulting from the difference in the angular velocities of the primary solids subdisc and the gas disc did not prevent gravitational instability which increases the concentration of solids. A condition for the development of instability is determined by the compression of the solid phase subdisc towards the star, in the equatorial plane. Such compression increases the ratio of the mass densities of the solid component and the gas by a factor of 2-10. The density of the medium in these regions starts to grow under the action of a self-gravitational field. Marov et al. (2008) noted that the possibility of a local concentration of bodies should be considered; this local concentration may result from the differential rotation of the gas subdisc in large turbulent structures. According to Cuzzi et al. (1993), such bodies will be represented by metre-sized boulders, since solids exceeding 1 m in size settle most efficiently on the equatorial plane. Meanwhile, smaller agglomerates are removed from this plane by a turbulent flow that results from the different angular velocities of the gas and solid-phase subdiscs.

Overall, the problem of planetesimal formation from primary solids, boulders and agglomerates in medium-mass quasi-stationary discs has not yet been convincingly solved. We therefore examined the possibility of planetesimal formation in the intermediate period between the existence of the massive accretion disc (age of more than 0.1 million years, with the mass of the disc comparable to the mass of the central body) and the medium-mass disc (age of more than 1 million years, with the mass of the disc approximately 10 times smaller than the mass of the central body).

For massive disc formation Machida, Inutsuka & Matsumoto (2008) simulated the structure of the gas flow and demonstrated that the streams outside the disc plane along the rotation axis must exist. These outgoing flows can provide intense non-radiative cooling of gaseous disc under the condition of weak radiative heating from protostar of a small mass.

Johansen et al. (2007) investigated local gravitational collapses in medium of sub-metre-sized solids in the disc. In their simulations the dispersion in the velocities of such solids was determined by turbulent fluctuations in the gas flow. Owing to the primarily collective motion of the gas and solids, the dispersion may be as high as ten metres per second. Johansen et al. (2007) found that in a local region with a self-gravitating medium and an external gravitational field exerted by a protostar, the drag force resulted in gravitational collapse in a subsystem of solids, over several orbital periods. Gas was not involved in such collapses. This mechanism was able to explain the growth of sub-metre-sized agglomerates into bodies with a size of 10 metres. These 10-metre-sized bodies experience rare but high-velocity collisions with each other during orbital time. In contrast to sub-metre-sized solids, drag forces do not cause such enlarged bodies to move in concert with gases. The collective motion of these bodies in the disc is described by the Vlasov equation.

The main thesis of this paper is that the gravitational interaction of the two phases (gases and primary solids over a metre in size) affects the stability of the entire disc, and changes the conditions necessary for the formation of clumps in such a system. We investigated the gravitational interactions between the gas and solid phases in a massive disc, during the development of an instability that could lead to

the formation of clumps. As it was explained above the surface density of the solid phase was assumed to be greater than 1 per cent of the gas surface density. The solids subdisc reaches its fragmentation threshold only due to presence of massive gaseous envelope.

The second section of the paper describes a mathematical model for the two-phase protoplanetary disc during clump formation, and the third section deals with the numerical algorithms and code we used in the computational experiments. The fourth section presents estimates for the effective Jeans lengths of the gravitational interactions between the gases and the primary solids subdisc. The fifth section shows the results of numerical modelling for the dynamics of the two-phase system with a central body, for time periods covering several disc rotations.

2 A MATHEMATICAL MODEL OF THE PROTOPLANETARY DISC DURING CLUMP FORMATION

2.1 Basic equations

The computational experiments reported in this paper were carried out within a quasi-3D model of the disc. This means that we neglected the vertical motion of matter, and considered the dynamics of the razor-thin disc where its entire mass was concentrated inside the equatorial plane of the system. The gravitational potential of the *multiphase* disc was calculated using the 3D Laplace equation.

The limits of such model applied to the disc description were discussed in detail by Fridman & Khoruzhii (2003). They found that the model is valid, first, when the typical length of density perturbation in the disc is greater than its thickness; secondly, when the changes of the dynamical processes time are slow with respect to orbital time. The first condition is satisfied for all process in the disc except for its collapsing. The second condition is satisfied for gravitational instability almost everywhere inside the disc except for its outer edge where dynamical and orbital time are comparable.

The gas component was described by the following gas dynamics equations:

$$\begin{aligned} \frac{\partial \sigma}{\partial t} + \text{div}(\sigma \mathbf{v}) &= 0, \\ \sigma \frac{\partial \mathbf{v}}{\partial t} + \sigma(\mathbf{v}, \nabla) \mathbf{v} &= -\nabla p^* - \sigma \nabla \Phi, \\ \frac{\partial S^*}{\partial t} + (\mathbf{v}, \nabla) S^* &= 0, \quad p^* = T^* \sigma. \end{aligned}$$

These gas dynamics equations include surface quantities that were obtained from volume quantities by integration with respect to the vertical coordinate z :

$$\sigma = \sigma_{gas} = \int_{-\infty}^{+\infty} \rho_{gas} dz; \quad p^* = \int_{-\infty}^{+\infty} p dz.$$

Here, $\mathbf{v} = (v_x, v_y)$ is the two-component gas velocity, and p^* is the surface gas pressure. $T^* = \frac{p^*}{\sigma}$, $S^* = \ln \frac{T^*}{\sigma^{\gamma^*-1}}$ are the quantities similar to gas temperature and entropy. γ^* is a 2D version of γ (Polyachenko & Fridman 1976), which is

related to the constant ratio of specific heats as $\gamma^* = 3 - \frac{2}{\gamma}$. Φ - is the gravitational potential in which the motion occurs.

In our model, the solid-phase subdisc was represented by 1-10 m solids moving in such a manner that two solids collided with a frequency not exceeding one event per rotation around the protostar. The dynamics of the primary solids subdisc were described by the Vlasov equation, neglecting collisions between solids at times longer than several rotations:

$$\frac{\partial f}{\partial t} + \mathbf{u} \frac{\partial f}{\partial \mathbf{r}} + \mathbf{a} \frac{\partial f}{\partial \mathbf{u}} = 0,$$

where $\mathbf{a} = -\nabla \Phi$, \mathbf{a} is the acceleration of particles in an external and self-consistent field, $\mathbf{u} = (u_r, u_\phi)$ is the two-component velocity of the particles, and $f = f(t, \mathbf{r}, \mathbf{u})$ is a function of the particle velocity distribution \mathbf{u} at a point in the disc with the coordinate \mathbf{r} . This function is related to the surface density of the particles as $\sigma_{par} = \int f d\mathbf{u} dz$. Note that the radius of the solids does not appear explicitly in the Vlasov equation; however, the description of the primary solids subdisc as a collisionless system implies a certain size range for these solids.

Φ is the gravitational potential, which is the sum of the potential of the motionless central body and the potential of the razor-thin disc, $\Phi = \Phi_1 + \Phi_2$, $\Phi_1 = -\frac{M_c}{r}$, where M_c is the mass of the central body. Φ_2 is the potential of the self-consistent gravitational field, which is defined in general from the Dirichlet problem for the 3D Poisson equation

$$\Delta \Phi_2 = 4\pi(\rho_{par} + \rho_{gas}), \quad \Phi_2 \longrightarrow \sqrt{r^2 + z^2} \rightarrow \infty \quad 0.$$

For $\rho_{par} + \rho_{gas} = (\sigma_{par}(r, \phi) + \sigma_{gas}(r, \phi))\delta(z)$, where $\delta(z)$ is the Dirac delta function, Φ_2 is found as a solution of mixed problem for the Laplace equation

$$\Delta \Phi_2 = 0, \quad \Phi_2 \longrightarrow \sqrt{r^2 + z^2} \rightarrow \infty \quad 0,$$

$$\frac{\partial \Phi_2}{\partial z} \Big|_{z=0} = 2\pi(\sigma_{par}(r, \phi) + \sigma_{gas}(r, \phi)).$$

The equations are written using dimensionless variables. The basic dimensional quantities are G (the gravitational constant), and $R_0 = 10$ au, $M_0 = M_\odot = 2 \cdot 10^{30}$ kg, which are the typical size and mass of the system. The gas component and the boulders subdisc interact through a common gravitational field.

2.2 Initial conditions

The surface temperature and density of the disc were specified at zero time. In the calculations presented in this paper, the density of the gas and primary solids subdisc was taken as a Mackloren disc of mass $M_{par,gas}$ and radius R :

$$\sigma_{par,gas}(r) = \begin{cases} \frac{3M_{par,gas}}{2\pi R^2} \sqrt{1 - (\frac{r}{R})^2}, & r < R, \\ 0, & r \geq R. \end{cases}$$

The gas temperature at zero time was specified as $T^*(r) \sim (1 - \frac{r}{R})$ or $T^*(r) \sim \sigma(r)$, using a given T_0 , which is the temperature in the 'centre' of the disc.

The initial velocities of the solids were specified as the sum of regular and random components, $\mathbf{u} = \mathbf{u}' + \mathbf{u}''$, where

\mathbf{u}' is the regular velocity, and \mathbf{u}'' is the random velocity. The gas velocity and the regular velocity of particles were determined from an equilibrium between centrifugal and centripetal gravitational forces: $\frac{v_\phi^2}{r} = \frac{1}{\sigma} \frac{\partial p^*}{\partial r} + \frac{\partial \Phi}{\partial r}$, $\frac{u_\phi'^2}{r} = \frac{\partial \Phi}{\partial r}$, where $v_r = 0$, and $u_r' = 0$. The random velocity of the particles \mathbf{u}'' was specified by the Gaussian law with a zero average and a prescribed dispersion v_d .

3 NUMERICAL METHODS AND SETUPS

We carried out our computer simulation of protoplanetary disc dynamics using a Sombrero code based on the method of splitting with respect to the physical processes involved (Stoyanovskaya & Snytnikov 2010). The Vlasov equation, the gas dynamics equations, and the mixed problem for the Laplace equation were solved at each time step.

The solution of the Vlasov equation was obtained using the particle-in-cell (PIC) method (Hockney 1987). We combined it with the grid method solution of the Laplace equation. We interpolated the surface density of solid bodies on the regular polar grid using the PIC kernel. The equations of each particle motions are characteristics of the Vlasov equation: $\frac{d\vec{u}}{dt} = -\nabla\Phi$, $\frac{d\vec{r}}{dt} = \vec{u}$. They were integrated by leap-frog scheme (Snytnikov et al. 2004).

The gas dynamics equations were solved using the SPH method (Monaghan 1992). The SPH calculation formulas implemented in Sombrero were obtained from quasi-3D gas dynamics equations, written in the Lagrangian form:

$$\frac{d\sigma}{dt} = \sigma \cdot \text{div} \mathbf{v}, \quad \frac{d\mathbf{v}}{dt} = -\frac{1}{\sigma} \nabla p - \nabla \Phi, \quad \frac{d\mathbf{r}}{dt} = \mathbf{v}, \quad \frac{dS}{dt} = 0,$$

where $\frac{d}{dt} = \frac{\partial}{\partial t} + \mathbf{v} \cdot \nabla$.

We used the cubic spline for 2D space as a kernel W :

$$W(q, h) = \frac{5}{14\pi h^2} \begin{cases} [(2-q)^3 - 4(1-q)^3], & 0 \leq q \leq 1, \\ [2-q]^3, & 1 \leq q \leq 2, \\ 0, & q > 2, \end{cases}$$

where $q = \frac{|\mathbf{x}|}{h}$, \mathbf{x} - radius vector of a space point.

The surface density of the gas where the i th particle resides was calculated as the sum interpolant $\sigma_i = \sum_{j=1}^N m_j W_{ij}$, where N was the number of simulated SPH particles. We used the adaptive smoothing length $h_i = 2\sqrt{\frac{m_i}{10^{-3} + \sigma_i}}$, which was implemented through arithmetic kernel averaging

$$W_{ij} = \frac{1}{2} (W(|r_i - r_j|, h_i) + W(|r_i - r_j|, h_j)).$$

The equation of motion was approximated such that the impulse and angular momentum were preserved:

$$\frac{d\mathbf{v}_i}{dt} = - \sum_j m_j \left(\frac{p_j}{\sigma_j^2} + \frac{p_i}{\sigma_i^2} + \Pi_{ij} \right) \nabla_i W_{ij} - \nabla \Phi_i,$$

$$\Pi_{ij} = \begin{cases} \frac{-\alpha \overline{c_{ij}} \mu_{ij} + \beta \mu_{ij}^2}{\overline{\rho_{ij}}}, & v_{ij} r_{ij} < 0, \\ 0, & v_{ij} r_{ij} \geq 0, \end{cases}$$

$$\mu_{ij} = \frac{h_{ij} v_{ij} r_{ij}}{|r_{ij}|^2 + 0.01 h_{ij}^2}, \quad \overline{c_{ij}} = \frac{1}{2} (c_i + c_j), \quad \overline{\sigma_{ij}} = \frac{1}{2} (\sigma_i + \sigma_j),$$

$$h_{ij} = \frac{1}{2} (h_i + h_j), \quad v_{ij} = v_i - v_j, \quad r_{ij} = r_i - r_j.$$

For calculation formulas we used notations:

$$W_{ij} = W(|r_i - r_j|, h), \quad \nabla_i W_{ij} = \frac{x_i - x_j}{h} \frac{\partial W_{ij}}{\partial q}.$$

We used a standard artificial viscosity with parameters $\alpha = 1$, $\beta = 1$ (Monaghan 1992) in Sombrero code to make the calculation of shearing motion possible. In our model we used the entropy equation, which doesn't describe the shock waves. That is why we introduced an artificial viscosity to the motion equation only. The kinetic energy of gas decreased due to the viscosity on 10 per cent $100 \times 128 \times 100$ grid cells and 40000 SPH particles for the test calculation. The contribution of artificial viscosity is decreased by increasing number of SPH particles. Numerical experiments show that the velocity field in clumps is not affected by the number of SPH particles. If we change the model by direct artificial heating it provides significant increasing of gas temperature and the transition of its flow from supersonic to subsonic in the inner part of the disc.

The Laplace equation was solved using a cylindrical region of space, with its lower face determining the disc plane. The particles simulating the gas disc and the primary solids subdisc were located in this plane. The Laplace equation was solved for the entire volume of the cylinder, using a cylindrical coordinate system. A boundary condition fixing the potential to zero at infinity was transferred to the side surfaces of the cylinder and the upper edge of the calculated region at each time step, via the decomposition of the potential into multipoles (up to quadrupole moments). The radius of the calculated region was typically twice as large as the initial radius of the disc, and the height of the cylinder was chosen to be equal to the radius of the calculated region. The Laplace equation was solved using an iterative combined method, where a value from the previous time step was taken as an initial approximation. This method employed fast Fourier transforms in angular coordinates, combined with a successive block over-relaxation procedure (Snytnikov et al. 2004).

The gravitational force affecting the SPH and PIC particles was calculated by a linear interpolation of the force rate in the mesh points which was obtained from the *mid-plane* gravitational potential value.

Most of the calculations presented below were performed on a $100 \times 128 \times 100$ grid. The particles did not reach the boundary of the calculated region in any of our calculations. To verify that the changes observed in the solutions were due to the parameters for the low-mass component of the disc (and were not related to numerical effects), all calculations were performed using the same numerical algorithm parameters. The gas disc was represented by 4×10^4 SPH particles. In this case, the mass of the particles within the smoothing length did not locally exceed the corresponding Jeans mass (Bate & Burkert 1997). The primary solids subdisc was represented by 5×10^6 PIC particles. In the disc plane, the grid size was $[r, \phi] = 100 \times 128$ with 50×128 cells representing the disc at zero time. The average number of PIC particles in each cell in the disc plane was therefore 1000, which provided a ≤ 3 per cent fluctuation in the density and other calculated quantities.

The resolution requirements for multi-phase and single-component medium studies are similar. Usually the Jeans

length in gas and subdisc of solids is greater than a few grid cells and smoothing lengthes of SPH particles. In the next section we discuss existence of effective Jeans length for gas-solid bodies medium. Hereby we suppose that a maximum grid cell size and a smoothing length must be less than the effective Jeans length.

In addition, the applicability of the methods implemented in Sombrero for the simulation of the dynamics of axisymmetric and radial-azimuthal structures (that form in the two-phase medium of the gravitating disc) was verified; this was achieved by comparing the results of computational experiments performed using the SPH and FLIC methods (Stoyanovskaya & Snytnikov 2010). It was shown that the SPH method was able to reproduce nonlinear waves in the gas and collisionless solids medium, with shear and counter flows emerging in the system.

4 GRAVITATIONAL INSTABILITY IN A MEDIUM OF GAS AND COLLISIONLESS PRIMARY SOLIDS MEDIUM: ANALYTICAL EXPECTATIONS

The scale separating the growing and decaying perturbations in a gravitating medium is determined by the local Jeans length. The Jeans length is obtained from an analysis of the dispersion ratios, which gives an estimate of the minimum density perturbation in a system developing under the action of a self-gravitational field. The long-wave stability of a collisionless, flat layer was considered by Fridman & Polyachenko (1984). They demonstrated that the critical length of the wave is equal to

$$\Lambda_{par} = \frac{T_{par}}{G\sigma_{par}m_{par}} = \frac{v_d^2}{G\sigma_{par}}.$$

The vibrations of the incompressible gas layer (in the same long-wave approximation,) are expressed by the relationship

$$\Lambda_{gas} = \frac{T_{gas}}{G\sigma_{gas}\mu} = \frac{c_{gas}^2}{G\sigma_{gas}}.$$

Similar expressions for the critical extent of the distortions are available for the Toomre instability in a heterogeneous rotating disc. The dynamics of gases and collisionless primary solids under a common gravitational field (in the same long-wave approximation of a flat layer in a circumstellar disc, for perturbation of a potential $\tilde{\Phi}$ near the equatorial plane, in scale Λ) can be written as $\tilde{\Phi} \sim G(\sigma_{par} + \sigma_{gas})\Lambda$, where σ_{par} , and σ_{gas} are perturbations in the particle and gas surface densities. For rapidly growing waves (rapid compared with the rotation period around a protostar), with reference to

$$\frac{1}{\mu} T \frac{\widetilde{\sigma_{gas}}}{\Lambda} \sim \frac{\sigma_{gas} \tilde{\Phi}}{\Lambda}, \quad v_d^2 \frac{\widetilde{\sigma_{par}}}{\Lambda} \sim \sigma_{par} \tilde{\Phi},$$

one can obtain $\frac{1}{\Lambda} \sim \frac{1}{\Lambda_{par}} + \frac{1}{\Lambda_{gas}}$, or

$$\Lambda = \frac{\Lambda_{gas}}{1 + \frac{c_{gas}^2}{v_d^2} \frac{\sigma_{par}}{\sigma_{gas}}} = \frac{\Lambda_{par}}{1 + \frac{v_d^2}{c_{gas}^2} \frac{\sigma_{gas}}{\sigma_{par}}},$$

where $m_{par}v_d^2$ is a typical 'temperature' for the velocity distribution function of solids (neglecting motion perpendicular

to the disc plane), m_{par} is the mass of a solid particle, and T and μ are the temperature and molecular weight of the gas. Λ gives the critical wavelength for a two-component disc, the so-called effective Jeans length for a two-phase system.

Relation $Q = \sqrt{\frac{\Lambda_{Jeans}}{\Lambda_{rot}}} < 1$ gives the classical Toomre value for the gravitational instability in the rotating disc, where $\Lambda_{rot} = \frac{G\sigma_{gas}}{\Omega^2}$, Ω - epicyclic frequency. For multiphase disc $\sigma = \sigma_{par} + \sigma_{gas}$, which defines $\Lambda_{rot} = \frac{G(\sigma_{gas} + \sigma_{par})}{\Omega^2}$. Then, using the obtained value of effective Jeans length the Toomre parameter can be written as $Q = \sqrt{\frac{\Lambda_{par}\Lambda_{gas}}{\Lambda_{gas} + \Lambda_{par}} \frac{\Omega^2}{G(\sigma_{gas} + \sigma_{par})}}$.

Inside the disc, for a mixture of hydrogen and helium at a temperature $T \approx 300$ K, $c_s \approx 1000$ m s⁻¹. For $\sigma_{par}/\sigma_{gas} \approx 5 * 10^{-2}$ (a massive gas disc), and with a dispersion in the solid velocities of $v_d \approx 100$ m s⁻¹, the length Λ decreased 6-fold compared with Λ_{gas} ; for $v_d \approx 20$ m s⁻¹, a 100-fold decrease was observed. It was therefore shown that the presence of a second low-mass component could strongly decrease the effective Jeans length for the two-phase system Λ . By developing the aforementioned instabilities in its subsystem, the low-mass phase was able to facilitate the development of gravitational instability in the entire medium. The role of the gas was reduced to providing a drag force on individual solids; such friction decreased the velocity dispersion of the primary solids. The gas therefore served as a massive medium, in which density perturbations transferred from the primary solids subdisc could develop, and produce clumps. The physics of the process is similar to the cooling of heavy ions by light electrons (which move in concert with the heavy ions) that occurs in accelerator physics (Nikitin, Snytnikov & Vshivkov 2004).

5 COMPUTATIONAL EXPERIMENTS

We will now clarify how the gravitational interactions between the cloud of low-mass collisionless primary solids and the massive gas can affect the formation and development of structures in the self-gravitating disc, on its rotation around the central body. Three cases can be distinguished: first, structures can form and develop due to instabilities in the gas, and can subsequently involve primary solids in their dynamics. Second, structures can be initiated in the primary solids subdisc, and can remain there for their entire lifetime, without any noticeable effect on the gas. Third, structures can be generated in the gas, but under the development of 'two-phase' instability, where the overall dynamics of the gas are affected by the low-mass primary solids subdisc.

The last mode is the most interesting; we will demonstrate that the 'two-phase' system (gas containing a subdisc that has low solid velocity dispersions) can act as a source of the instability necessary for the formation of self-gravitating gas-solid clumps in the disc.

In order to demonstrate that all three modes exist in massive protoplanetary discs, we reproduced the dynamics of some rotations of a disc with mass $M = 0.55M_0$ and radius $R = 2R_0 = 20$ au, rotating around a central body with mass $M_c = 0.45M_0$. It should be noted that when going from a 3D disc to its quasi-3D approximation, we retained a

Table 1. Parameters and corresponding Jeans lengths for computational experiments.

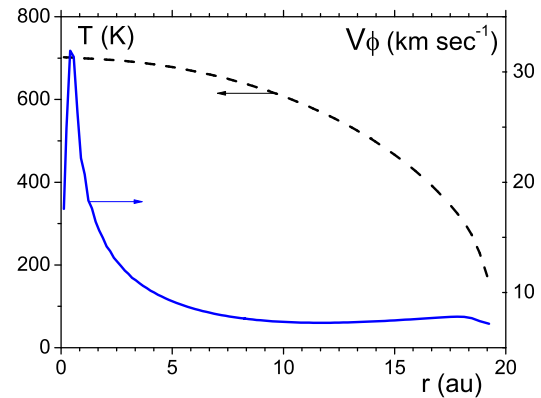
Experiment No	1	2	3	4
Mass of gas	$0.52M_0$	$0.495M_0$	$0.52M_0$	$0.52M_0$
Mass of solids	$0.03M_0$	$0.055M_0$	$0.03M_0$	$0.03M_0$
Initial gas temperature at $R = 10$ au (K)	610	1335	610	610
Initial velocity dispersion of solids (m s^{-1})	1900	285	475	95
Initial Jeans length in gas	0.42	0.97	0.42	0.42
Initial Jeans length in solids at $R = 1$ au	6.45	0.2	0.4	0.016
Outcome of instability development	3 spiral arms in gas and solids	10 spiral arms in solids transformed into 3 spiral arms in gas and solids. Thermalization of solids	5 spiral arms in gas and solids	Gas-solid clumps in the inflection points of 5 spiral arms

fixed ratio between the masses of the central body and the disc, M_c/M . All calculations reported in this paper used $\gamma^* = 5/3$. The ratio of the surface densities of the primary solids subdisc and the gas disc ($\sigma_{par}/\sigma_{gas}$) was varied in the range of 0.01 - 0.1. This differed from the ratio between the solid and gas phases in molecular clouds (which has a value between 0.01 and 0.02), due to the accumulation of the solid phase in the disc, and the greater thickness of the gas subdisc compared with the solids subdisc. In the quasi-3D model, $\sigma_{par}/\sigma_{gas} = m_{par}/m_{gas}$. By specifying the ratio of the surface densities and the mass of the entire disc, we determined the masses of the gas and the primary solids subdisc. Thus, in calculations 1, 3, 4 (Table 1), the mass of gas in the disc was $M_{gas} = 0.52M_0$, and the mass of the particles was $M_{par} = 0.03M_0$, which corresponds to the surface density ratio $\sigma_{par}/\sigma_{gas} \approx 0.058$. In contrast, in calculation 2, $M_{gas} = 0.495M_0$ and $M_{par} = 0.055M_0$, which gave a surface density ratio of $\sigma_{par}/\sigma_{gas} \approx 0.11$.

We specified the density and temperature (dispersion) of the disc to give an initial state of unstable equilibrium. Such a choice of initial state made it possible to follow the main stages of the development of instability in the calculations. The initial gas temperature and solid velocity dispersion conditions were set to provide a certain level of instability in each component of the disc. Table 1 provides a summary of the parameters and corresponding Jeans lengths for each run. Fig. 2 (which shows the initial radial distributions of the temperature and angular velocity in the gas, for experiment 1) shows that ultrasonic gas flow with differential rotation was reproduced.

Experiment 1 was run in a mode where the formation of the disc structure was determined by the gas, while the gravitational field of the massive component meant that the solids were also involved in the structures. In this run, the initial Jeans length Λ for the gas (which was constant over the entire disc) was equal to 0.42, which corresponded to a gas temperature profile $T^* \sim \sigma_{gas}$. For such a dependence, at a radius $R = 10$ au the temperature was 610 K; at a radius $R = 1$ au, the temperature was 700 K. The Jeans length in the primary solids subdisc increased from the centre to the periphery, and reached 6.45 at $R = 1$ au, due to an initial primary solids velocity dispersion of $v_d = 1900 \text{ m s}^{-1}$.

Values for the Toomre parameter $Q = \frac{c_s \kappa}{\pi G \sigma}$ (which characterises the level of gravitational stability of a rotating flat disc, and where $\kappa \approx \Omega$ for discs with near-Keplerian ro-


Figure 2. Gas temperature and angular velocity versus radius at initial time, for experiments 1, 3, and 4

tation) are shown in Fig. 3 for calculations 1, 3 and 4, for gases and primary solids. At a specified gas mass and temperature, a value of $Q < 1$ corresponded to the disc region $R > 2$ au, which indicated that the radial-ring instability could develop in the gaseous disc.

As shown in Fig. 4 in the images from Run 1 (the images show the surface densities of the gas and particles), broad density rings had formed in the gaseous disc and on its periphery by the time $t = 10$. The density distribution of solids was similar to that in the gas, except for the narrow solid density rings at a radius of ≈ 8 au. By the time $t = 15$, azimuthal instability had developed, resulting in the formation of a three-arm spiral structure in the gas. The width of the solid spirals was much smaller than the width of the gas spirals. The solids concentrated in the spiral gas arms formed their own structure, which was thinner than the gas structure. At a later time of $t = 23$, this relatively thin solid structure disappeared, leaving a well developed three-arm structure; in this case, the dynamics of the disc were determined by the gas. Therefore, for high initial velocity dispersions, the bodies showed neither large inhomogeneities in their density nor any significant thermalisation of velocities, leading to a smooth spiral structure that covered the solids; this was the result when the disc dynamics were determined almost completely by the massive gas component.

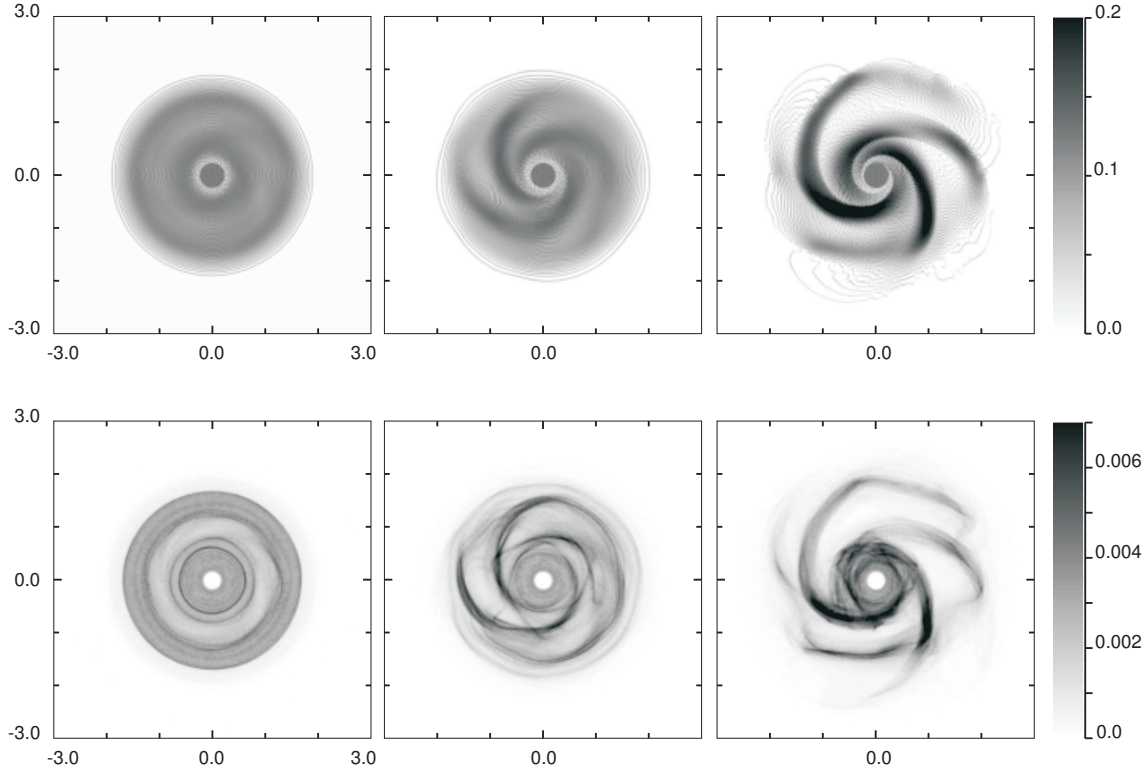


Figure 4. : The formation of spiral arms due to the development of gravitational instability in the gas. The surface density of the gas (top) and the primary solids subdisc in experiment 1, for time points $T = 10, 15$, and 23 .

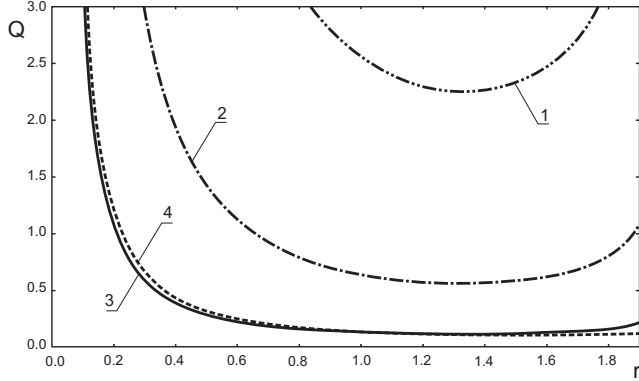


Figure 3. Initial value of the Toomre Q parameter versus radius, for experiments 1, 3, and 4. 1, 2, and 3 show curves for the primary solids subdisc: 1 - experiment 1 (corresponding to an initial thermal velocity $v_d = 1900 \text{ m s}^{-1}$), 2 - experiment 3 ($v_d = 475 \text{ m s}^{-1}$), 3 - experiment 4 ($v_d = 95 \text{ m s}^{-1}$). 4 - gas curve corresponding to all three experiments.

The benchmark Run 2 — where the gas temperature increased more than twofold, and the solid velocity dispersion decreased by a factor of almost 7 compared with Run 1 — showed radically different disc dynamics. This run corresponded to the second case considered above for the interaction between the particles and gas. For such disc parameters, the effective Jeans length Λ was determined by the primary solids subdisc, as illustrated in Fig. 5. By $t = 10$, a strong azimuthal instability had developed in the low-mass component of the disc, resulting in the formation of numerous

spiral arms. Radial-ring structures in the solid disc were revealed in the gas. By $t = 20$, further interactions between the spiral waves in the solid phase had produced a distinct ten-arm structure in the outer part of the subdisc, and a complex wave structure in the interior of the subdisc. Such structures were generally absent in the gas component. The function $\Delta N = \frac{\partial N}{\partial v_r} \Delta v_r$, where N - the velocity distribution function of solids, (see Fig. 6) remained almost unchanged for $t = 20$. By $t = 30$ (which roughly corresponded to the next disc rotation over the periphery), the solids were scattered in patterns determined by their density waves, with their distribution function showing an increase of nearly an order of magnitude. Such a distribution function corresponded to a 3- to 4-arm density of solids in the disc (see Fig. 5) and weakly revealed structures in the gas. The number of particles with significantly lower velocities (obeying the distribution function $dv < -0.4$) was still increasing, as was the number of solids with slightly higher velocities (with $dv < 0.2$); by $t = 50$, the disc composed of both solids and gas attained an equilibrium thermalised state. Thus, for this run, the thermalisation time of the disc (whose instability was higher in the solid component than in the gas) was smaller than the time taken for the solid subdisc to decay into separate clumps, under Jeans instability working against a moving but uninvolved gas.

Experiments 3 and 4 showed the development of two-phase gravitational instability, with both the massive gas component of the disc and the primary solids subdisc influencing the formation of structures. The disc dynamics calculations were performed using gas parameters similar to

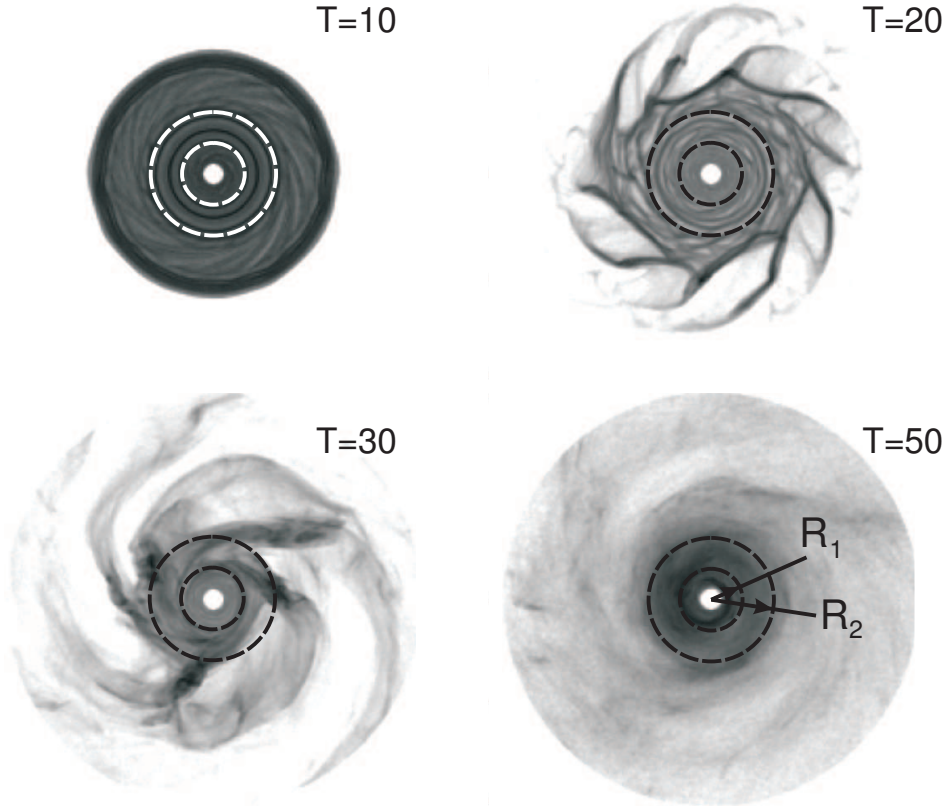


Figure 5. The formation of structures and the development of gravitational instability in a mode where the value of the Toomre parameter for the primary solids subdisc was lower than that for the gas. Logarithm of the primary solids subdisc surface density, for time points $T = 10, 20, 30$, and 50 , for experiment 2.

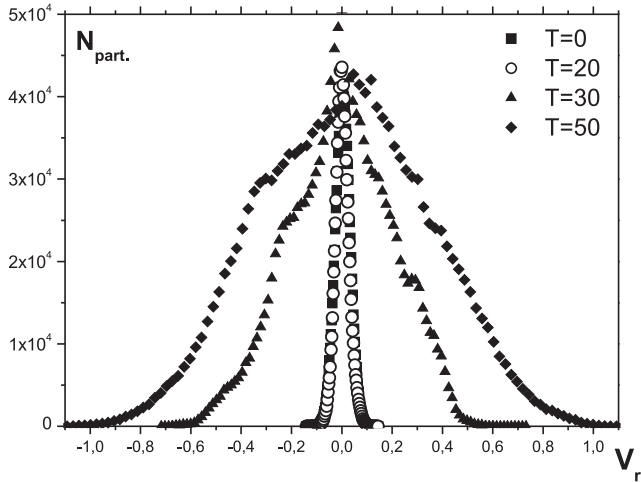


Figure 6. Function $\Delta N = \frac{\partial N}{\partial v_r} \Delta v_r$, where N —the velocity distribution function of PIC particles in a solid subdisc residing in a ring $[r_1, r_2] = [0.45, 0.9]$, for time points $T = 0 \ \Delta v_r = 0.0033$, $T = 20 \ \Delta v_r = 0.007$, $T = 30 \ \Delta v_r = 0.011$, $T = 50 \ \Delta v_r = 0.013$, in experiment 2.)

those used in experiment 1; the only change was that the primary solids velocity dispersion was decreased to 475 m s^{-1} in experiment 3, and 95 m s^{-1} in experiment 4.

In Fig. 7, for Run 3, the density distribution in the gas-

solid subdisc indicated that the development of this process in a gas with a colder low-mass component produced a 5-arm structure instead of a 3-arm one, after the same amount of time. The lateral linear dimensions of the individual density waves in the solids spiral (i.e., the thickness of these entities) were much smaller than those obtained in experiment 1 for the spiral waves formed mainly by the gas component. Such a decrease in the thickness of the solid 'filaments' also took place in the radial-ring structure on the disc periphery, which was less clear for the gas. The peripheral structure of the solids was characterised by a strong interaction with the spiral waves in the middle of the disc, which led to the breakdown of the azimuthal symmetry. This interaction produced high-density zones, due to the coupling between the particles and gas in the radial-ring and spiral-wave domains. This result raises the possibility that self-gravitation sufficient to oppose thermalisation factors in the two-phase disc may be triggered in such zones.

In order to assess this possibility, let us consider the results of experiment 4, where the solid velocity dispersion was decreased again by a factor of 5, to approximately $0.1 c_s$. In this case, the spiral structure did not change, and the spiral retained its full number of arms. This confirmed the importance of the role of the massive and unstable gas disc in the appearance of the spiral structure. However, over a narrow range, the number of arms depended on the solid subdisc parameters. The thickness of the solid-phase arms decreased significantly in comparison with experiment 3. In

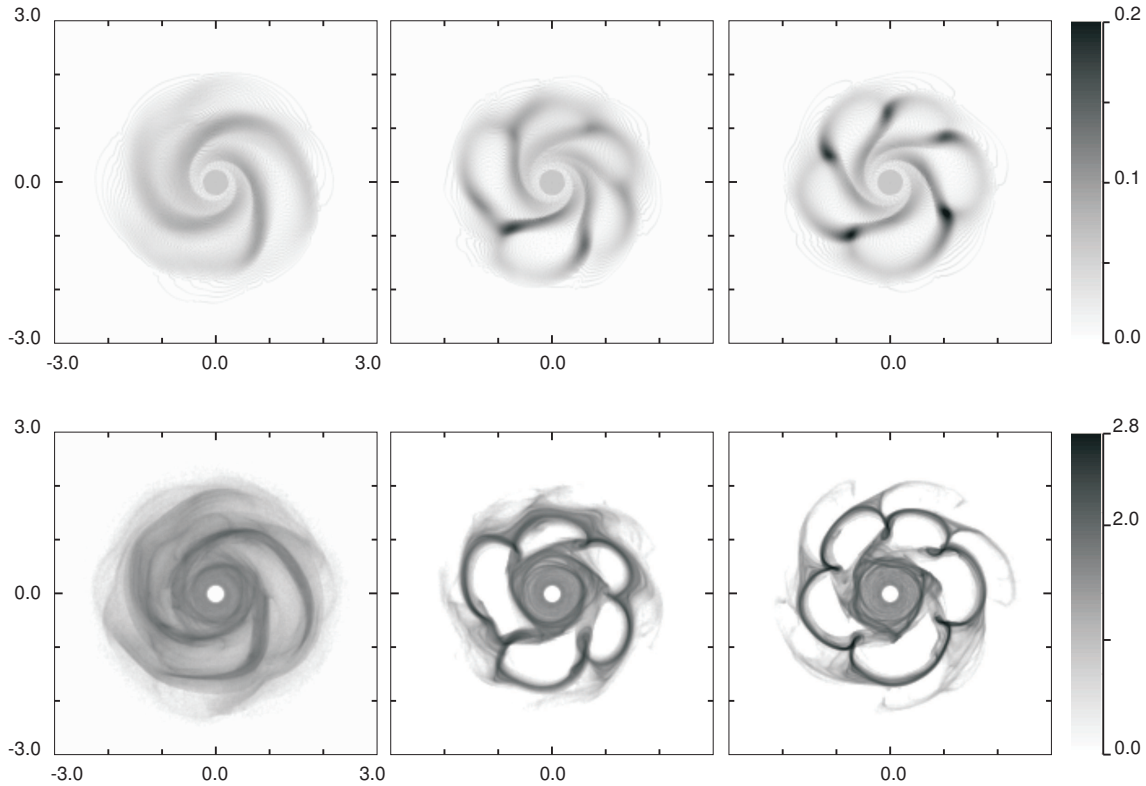


Figure 7. The surface density of gas (top) and the logarithm of the surface density of the primary solids subdisc, for experiments 1, 3, and 4, for time points $T = 20, 19$, and 22 , respectively.

the radial-ring and spiral-wave coupling region, more clumps were formed with high densities of both solid and gas. Here, the solid phase density exceeded the background values by a factor of at least ten. The clumps formed in the regions of minimum Jeans length. Thus, the development of instabilities in the two-phase disc resulted in the formation of five areas of increased gas-solid density, with a possible subsequent local gravitational collapse of gas and solids. There was insufficient time for the scattering of solids by density waves to occur in these regions; the time was also not sufficient for the primary solids subdisc to experience complete thermalisation, or to pass out of its quasi-equilibrium state. This conclusion neglects the drag force between gas and solids, an assumption that is valid for some tens of rotations. At long times, drag due to the gas should be taken into account, as it can decrease the velocity dispersion of solids at a certain radius from the central body.

To make sure that fragmentation in experiment 4 is not a numerical artefact we calculated this regime with increasing numerical resolution. We consequently increased the number of SPH and PIC particles four times and the number of meshpoints twice in each direction. Fig. 8 shows the surface density of gas and solid bodies in linear and logarithmic scale respectively. The spiral structure is formed almost simultaneously in calculations with increasing numerical resolution. We calculated the development of physical instability. Generally it shows a discontinuous dependency of solution on problem parameters (Vshivkov, Nikitin & Snytnikov, 2003). So details in density plots are changed with the numerical resolution variation, when the picture almost remains. All plots demonstrate the appearance of gas

clumps bound with solid clumps. Increasing the number of PIC and SPH particles and meshpoints allowed us to reproduce the wave interaction of the structures with the groups of particles.

These results can be used to explain the mechanism by which gas giants are formed. The formation of gas clusters due to gravitational instability has been considered to be a possible mechanism for the formation of Jupiter and Saturn (Boss 2000). However, the separate fragmentation of the gas disc was feasible (in computational experiments) only under strong cooling of the system during several rotations (Boss 2000, Durisen et al. 2007, Rice et al. 2006, Meru & Bate 2010). Our calculations demonstrated that in a two-phase gravitating medium, the low-mass part of the disc (composed of metre-sized solids) could initiate and accelerate the gravitational growth of waves in both components of the system, for the case of low solid velocity dispersions.

6 CONCLUSIONS

In this study, we examined a major bottleneck in the understanding of the process of planet formation; namely, the formation of large bodies (planetesimals and planet embryos) from metre-sized boulders in the circumstellar disc. A planetesimal in its emergent stage is considered as a clump of gas and solids whose gravitational field preserves its mass when the clump moves. We have proposed a mechanism that can explain the formation of planetesimals in massive accreting discs: in this emergent stage, the mass of a protostar is almost equal to the mass of the circumstellar disc. Gas leaves

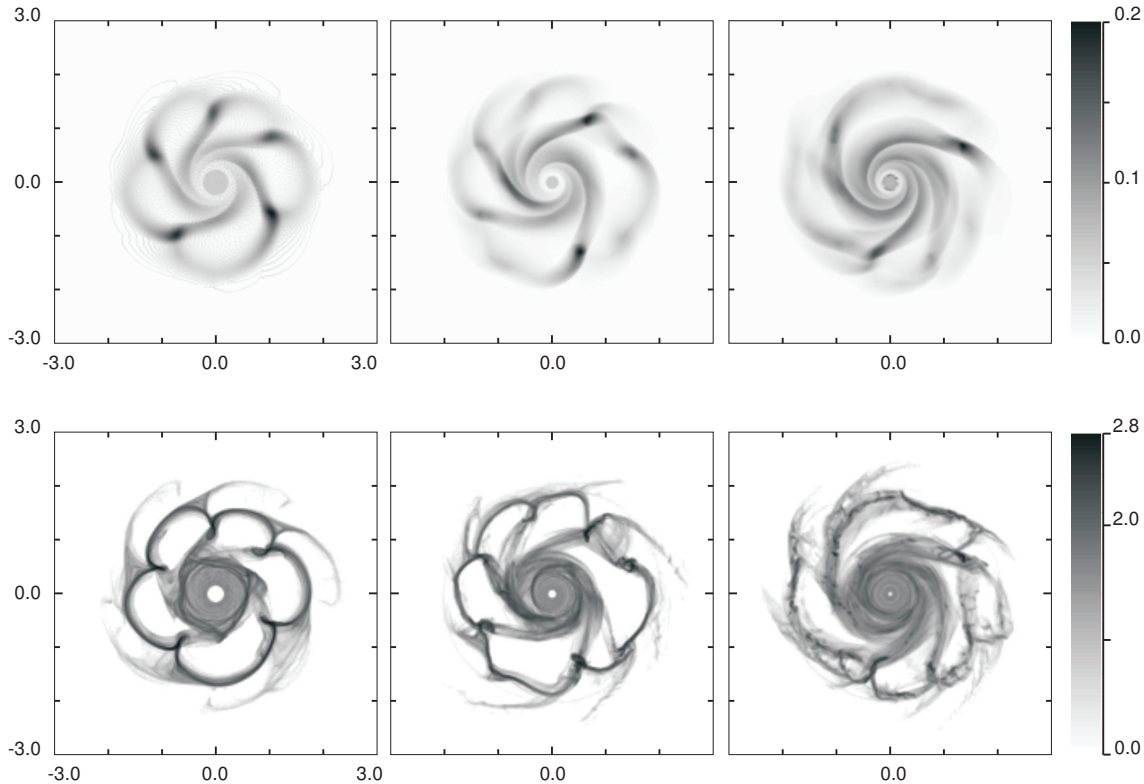


Figure 8. The surface density of gas (top) and the logarithm of the surface density of the primary solids subdisc, for experiment 4 with varying numerical resolution, for time points $T = 22, 23$, and 23 , respectively. The left column - 40000 SPH particles, 2500000 PIC particles, $100 \times 128 \times 100$ grid cells, the middle column - 160000 SPH particles, 10000000 PIC particles, $200 \times 256 \times 200$ grid cells, the right column - 640000 SPH particles, 40000000 PIC particles, $400 \times 512 \times 400$ grid cells.

the solid subdisc, being reflected from the equatorial plane, and is scattered to outer space. The gas temperature drops during this process, under conditions of low radiation from the low-mass protostar. Solid bodies grow to metric size with the occurrence of collisions, and lose relative velocity due to gas drag. In general, the solid component stays in the equatorial plane of the disc, while the gas leaves it. The fraction of the solid component therefore increases with respect to the gas. The increasing solid density, in combination with the decreasing gas temperature, causes the two-phase disc to transfer into a marginal state, allowing the development of gravitational instability of some type.

Our computer simulation showed that self-gravitating clumps were formed in a massive disc via the development of a 'two-phase' Jeans instability in the gas-primary bodies medium. These bodies were of larger than metre-sized, and rotated around the protostar without the occurrence of collisions per orbital time. In these unstable conditions, the overall gas dynamics were affected by the primary solids subdisc, via its gravitational field. This implied that the possibility of clump formation was determined both by the rate of gas cooling and its density redistribution, and by the rate of concentration of large (over 1 m) primary solids, and the decrease in their velocity dispersions (cooling of primary solids). We found that a velocity dispersion of $0.1 c_s$ in the boulder subdisc was sufficient to cause the formation of self-gravitating clumps of gas and boulders. In such regimes, the time taken for the formation of collapsing objects was

less than time taken for boulders to dissipate in the density waves of the medium.

ACKNOWLEDGMENTS

We would like to thank the anonymous referee, whose constructive comments led to an improvement of the paper. Our work was supported by the RAS Presidium programs 'Biosphere origin and evolution' and 'Origin, structure and evolution of objects in the Universe', as well as SB RAS Integration Project No. 26 'Mathematical models, numerical methods and parallel algorithms for solving big problems of SB RAS and their implementation on multiprocessor supercomputers', and Russian Federation President Grant for the Leading Scientific Schools NSh 3156.2010.3.

REFERENCES

- Armitage P.J., 2006, Lecture notes on the formation and early evolution of planetary systems (Based on lectures given at the University of Colorado, Boulder, in Fall 2006), arXiv:astro-ph/0701485v1
- Bate M. R., Burkert A., 1997, MNRAS, 288, 1060
- Boss A.P., 2000, ApJ, 536, 101
- Clarke C. J., Harper-Clark E., Lodato G., 2007, MNRAS, 381, 1543
- Cuzzi J.N., Dobrovolskis A.R., Champney J.R., 1993, Icarus, 106, 102

- Cuzzi J.N., Weidenschilling S.J., 2006, *Meteorites and the Early Solar System II* (ed. Lauretta D.S., McSween H.Y.). University of Arizona Press. 353
- Durisen R.H., Boss A.P., Mayer L., Nelson A.F., Quinn T., Rice W.K.M., 2007, *Protostars and Planets V*. B. Reipurth, D. Jewitt, and K. Keil (eds.). Univ. of Arizona Press, Tucson
- Edgeworth K. E., 1949., *MNRAS*, 109, 600
- Fridman A.M., 2008, *Adv. Phys. Sci.*, 178, 225
- Fridman A.M., Khoruzhii O.V., 2003, *Space Sci. Rev.*, 105, 1
- Fridman A.M., Polyachenko V.L., 1984, *Physics of Gravitating Systems, Vol.1 Equilibrium and Stability*. Springer Verlag, New York, Berlin, Heidelberg, Tokyo
- Gammie C.F., 2001, *ApJ*, 553, 174
- Goldreich P., Ward W.R., 1973, *ApJ*, 183, 1051
- Gurevich L.E., Lebedinskiy A.I., 1950, *Doklady Akademii Nauk*, 74, 673
- Hartmann L., 2009, *Accretion Process in Star Formation*. Cambridge University Press.
- Herbst E., van Dishoeck E.F., 2009, *ARA&A*, 47, 427
- Hockney R., Eastwood J., 1987, *Computer Simulation Using Particles*, Mir, Moscow
- Johansen A., Oishi J.S., Mac Low M.-M., Klahr H., Henning T., Youdin A., 2007, *Nat*, 448, 1022
- Khassin A.A., Snytnikov V.N., 2005, *Abstracts, International Workshop Biosphere Origin and Evolution*, Boreskov Institute of Catalysis SB RAS, Novosibirsk, 158
- Landau L.D., Lifshitz E.M., 1987, *Fluid Mechanics (Course of Theoretical Physics, Volume 6)*. Butterworth-Heinemann
- Levin B.Yu., 1964, *Origin of Earth and planets*. Nauka, Moscow
- Lodato G., Clarke C. J., 2011, *MNRAS*, 413, 2735
- Lodders K., Fegley B., 1998, *The Planetary Scientist's Companion*. Oxford University Press, N.Y.-Oxford.
- Machida M.N., Inutsuka S, Matsumoto T., 2008, *ApJ*, 676, 1088
- Makalkin A.B., Ziglina I.N., 2004, *Solar System Research*, 38, 330
- Marov M.Ya., Kolesnichenko A.V., Makalkin A.B., Dorofeeva V.A., Ziglina I.N., Chernov A.V., 2008, *Problems of Biosphere Origin and Evolution* (ed. Galimov E.M.). Librokom, Moscow. 329
- Mayer L., Quinn T., Wadsley J., Stadel J., 2004, *ApJ*, 609, 1045
- Meru F., Bate M. R., 2010, *MNRAS*, 410, 559
- Monaghan J.J., 1992, *ARA&A*, 30, 543
- Nikitin S.A., Snytnikov V.N., Vshivkov V.A., 2004, *Plasmas in the laboratory and in the universe. New insights and new challenges*. Bertin G., Farina D., Pozzoli R. (eds.) Melville, New York, P. 280
- Orishich A.M., Ponomarenko A.G., Snytnikov V.N., 1989, *Journal of Applied Mechanics and Technical Physics*, 30, 509
- Petit J.-M., Morbidelli A., 2005, *Lectures in Astrobiology*. M. Gargaud et al. (Ed.). Vol. 1, P. 61
- Rafikov R. R., 2009, *ApJ*, 704, 281
- Rice W.K.M., Armitage P.J., Bate M.R., Bonnell I.A., 2003, *MNRAS*, 339, 1025
- Rice W.K.M., Lodato G., Pringle J.E., Armitage P.J., Bonnell I.A., 2004, *MNRAS*, 355, 543
- Rice W.K.M., Lodato G., Armitage P.J., 2005, 364, L56
- Rice W.K.M., Lodato G., Pringle J.E., Armitage P.J., Bonnell I.A., 2006, *MNRAS*, 372, 9
- Safronov V.S., 1969, *Evolution of preplanetary cloud and formation of Earth and planets*. Nauka, Moscow
- Snytnikov V.N., Vshivkov V.A., Kuksheva E.A., Neupokoev E.V., Nikitin S.A., Snytnikov A.V., 2004, *Lett. to Azh*, 30, 146
- Spitzer L. Jr, 1978, *Physical Processes in the Interstellar Medium*. John Wiley & Sons Inc
- Stoyanovskaya O.P., Snytnikov V.N., 2010, *Mathematical Modeling*, 22, 29
- Stoyanovskaya O.P., Snytnikov V.N., 2009, *Proceedings of the 4th SPHERIC Workshop*, Nantes, P.85
- Vshivkov V.A., Nikitin S.A., Snytnikov V.N., 2003, *JETP Letters*, 78, 358
- Weidenschilling S.J., 2000, *Space Sci. Rev.*, 92, 295
- Youdin A., Shu F., 2002, *ApJ*, 580, 494

This paper has been typeset from a \LaTeX file prepared by the author.